

## GALACTIC MODELS AND STELLAR ORBITS\*

J a a n E i n a s t o

Abstract. Methods of determination of composite models of galaxies are outlined. The available observational information renders it possible to distinguish the following populations in nearby galaxies: nucleus, kernel, core, bulge, halo, disc, young population. Parameters of models of six galaxies are presented (our Galaxy, M31, M32, M87, and dwarf galaxies in Fornax and Sculptor). New data indicate that galaxies have much higher degree of mass concentration to the centre than adopted in previous models, and that giant galaxies may be surrounded by massive gaseous coronae of very large dimensions.

Recent developments in derivation of stellar orbits and kinematical characteristics of various stellar populations in galaxies are also summarized.

In the last section models of physical and dynamical evolution of galaxies are discussed.

\* Invited Report, IAU Regional Meeting, Athens, September 1972.

## I Introduction

=====

The construction of models is the most effective tool for synthesis of various observational data and quantitative study of the physical and dynamical structure and evolution of stellar systems.

In earlier model studies the goal has been more specific, since the models have been considered mainly as mass distribution models only (Perek 1962).

Classical models of spiral galaxies are based on rotational velocities, which are identified with circular velocities. The models of elliptical galaxies are based on luminosity distribution. The mass distribution is found under the assumption that the mass-to-luminosity ratio is constant over the whole system. The latter quantity is determined from the virial theorem by means of the velocity distribution in the centre of the system.

Some years ago it became apparent that a new approach to the constructing of models of stellar systems is necessary. First of all, recent observational and theoretical data have raised serious doubts over the validity of the assumptions mentioned above. Secondly, present observational technique permits to study not only the general distribution of mass in galaxies, but also the dynamical and physical structure of different stellar populations in them. And finally, the study of physical and dynamical evolution of galaxies has become an important new branch of investigation. All these aspects must be taken into consideration in developing new methods of modelling of galaxies.

In the following we give a review of problems connected with the construction of spatial and kinematical models of galaxies, and describe shortly the corresponding procedures. New results on the structure and evolution of galaxies will be presented.

The spatial structure of galaxies and their populations is closely associated with properties of stellar motion. This aspect will be also discussed in connection with the problem of stellar orbits.

## II New observational data on galaxies

As mentioned above, new observational data enable us to study the distribution of stars of different populations in galaxies. Under a population we mean the family of stars or other objects, having similar physical properties (age, chemical composition etc.) and similar parameters of spatial distribution and kinematics. The population problem in galaxies has been recently reviewed by King (1971).

The most important new observational data, on which the study of populations is based, are the spectrophotometric and colorimetric data concerning the stellar content of galaxies.

Pioneering work in this direction has been made by Morgan and Mayall (1957), and Spinrad (1962). The first two authors discovered that the spectra of centres of M31 and giant elliptical galaxies have cyanogen bands of normal strength. This indicates that the majority of stars in central regions of these galaxies are old population I stars rather than metal-poor population II stars of globular-cluster type. Population II is also present there, but it is not the dominating population. Spinrad has found that in centres of giant elliptical and spiral galaxies the D lines of sodium are very strong which indicates the presence of red dwarfs in large number. Later McClure (1969) and Spinrad and Taylor (1971a) found that the lines of metals in the spectra of some old open clusters and nuclei of giant galaxies are also very strong. They interpret the results in terms of super-metal-rich nuclei of giant galaxies and old open clusters (Spinrad et al. 1970). Spinrad and his collaborators have developed methods of derivation of mass-to-luminosity ratios of galaxies on the basis of spectrophotometric data (Spinrad et al. 1971, Spinrad 1971, Spinrad and Taylor 1971b).

Spectrophotometric methods can be applied for central bright parts of galaxies only. Valuable information on star content of galaxies, including faint peripheral regions, can be obtained by photometric methods, using the metallicity parameter  $Q$  (van

den Bergh 1967) or other combinations of UBVRIJKL colours.

By means of large optical and radio telescopes the distribution of individual bright objects in nearby galaxies can be also studied. Among these objects we mention globular clusters, studied by Vetešnik (1962), Kinman (1963), Racine (1968), Sharov (1968a), van den Bergh (1969), and others, novae (Sharov 1968b), supernovae (Tammann 1970), emission nebulae (Baade, Arp 1964, Deharveng, Pellet 1969, Courtes et al. 1968), stellar associations (van den Bergh 1964), and neutral hydrogen (s. van Woerden 1967).

Parameters, characterizing the physical and dynamical structure of populations, cannot be determined directly from observations in all cases. For example, the mass-to-luminosity ratios of the bulge, the disc and the halo of a galaxy cannot be derived from spectrophotometric observations. This quantity can be estimated from models of evolution of galaxies.

### III Methods of construction of models of stellar systems

Under a model of a stellar system we mean a set of functions and parameters, describing the main features of the system, included the presence of populations in it. The main descriptive functions are the following: the gravitational potential  $\phi$  and its radial and vertical derivatives  $K_R$  and  $K_z$ , the spatial density of mass  $\rho$ , the projected (along the line of sight) density of mass  $P$ , the projected luminosity density  $L$ , velocity dispersions in cylindrical system of coordinates  $\sigma_R$ ,  $\sigma_\theta$ ,  $\sigma_z$ , the centroid velocity  $V_\theta$ , and inclination angle of the major axis of the velocity ellipsoid to the plane of the galaxy  $\alpha$ . All these functions are connected with each other by means of various equations; the form of the equations depends on certain assumptions on the shape of equidensity surfaces and on some other conditions.

To construct a model of a galaxy three problems are to be solved.

1. The choice of equations connecting the descriptive functions.
2. The choice of analytic form for the initial descriptive function.
3. The determination of parameters of descriptive functions.

To fix the form of connection equations we make two assumptions. First, we suppose that galaxies are in a steady state and are symmetrical in respect to the rotational axis and equatorial plane. Secondly, we suppose that galaxies consist of ellipsoidal components of different flattening that represent different stellar populations in them. These assumptions are a good approximation to real galaxies. The assumption on ellipsoidal distribution of mass has the advantage that the form of the connection equations is the simplest one (Einasto 1969a, 1969b, 1970a). For the projected density of a component we have

$$P(A) = fL(A) = \frac{f}{2\pi E} \int_A^{\infty} \frac{\mu(\alpha) d\alpha}{\alpha \sqrt{\alpha^2 - A^2}}, \quad (1)$$

where  $\alpha = \sqrt{R^2 + \varepsilon^2 z^2}$  is the semimajor axis of the equidensity ellipsoid with axial ratio  $\varepsilon$ ;  $R, z$  being cylindrical coordinates and  $A$  is the semimajor axis of the projected density ellipse with the apparent axial ratio  $E$ ,

$$E^2 = \sin^2 i + \varepsilon^2 \cos^2 i, \quad (2)$$

$i$  being the angle between the plane of the system and the line of sight. Further  $f$  is the mass-to-luminosity ratio of the component. According to our assumption  $f$  is constant over the whole component. Finally

$$\mu(\alpha) = 4\pi \varepsilon \alpha^2 \varrho(\alpha) \quad (3)$$

is the mass distribution function (the mass of an equidensity layer of unit thickness at the equator).

Gravitational potential and its gradients can be found from the following expressions

$$K_R(R, z) = R G \int_0^1 \frac{\mu(\alpha) u^2 du}{\alpha^2 [1 - (\epsilon u)^2]^{3/2}}, \quad (4)$$

$$K_z(R, z) = z G \int_0^1 \frac{\mu(\alpha) u^2 du}{\alpha^2 [1 - (\epsilon u)^2]^{3/2}}, \quad (5)$$

$$\Phi(R, z) = - \int_R^\infty K_R(R, z) dR = - \int_z^\infty K_z(R, z) dz, \quad (6)$$

where  $\alpha$  is connected with the integration variable  $u$  by the formula

$$\alpha^2 = u^2 (R^2 + z^2 [1 - (\epsilon u)^2]^{-1}). \quad (7)$$

If the galaxy consists of more than one component, at right hand side of (4) and (5) the corresponding sums are to be written.

Kinematical functions can be calculated by means of hydrodynamical equations of stellar dynamics

$$\frac{1}{R} (\sigma_R^2 - \sigma_\theta^2) + \frac{1}{\rho} \frac{\partial}{\partial R} (\rho \sigma_R^2) + \frac{1}{\rho} \frac{\partial}{\partial z} [\rho \gamma (\sigma_R^2 - \sigma_z^2)] - \frac{V_R^2}{R} = -K_R, \quad (8)$$

$$\frac{1}{R} \gamma (\sigma_R^2 - \sigma_z^2) + \frac{1}{\rho} \frac{\partial}{\partial R} [\rho \gamma (\sigma_R^2 - \sigma_z^2)] + \frac{1}{\rho} \frac{\partial}{\partial z} (\rho \sigma_z^2) = -K_z, \quad (9)$$

where

$$\gamma = \frac{1}{2} \operatorname{tg} 2\alpha. \quad (10)$$

If the galaxy has a composite structure, the total number of functions to be determined is large and the numerical integration of equations is impossible. The procedure used by most investigators is following: an analytic expression is adopted for one of the descriptive functions - this function can be called the initial descriptive function. Other functions will be calculated by means of formulae given above. The problem of determining of the model of a galaxy is reduced to the determination of the parameters of the initial descriptive function.

The spatial density  $\rho$ , projected density  $P$  or gravitational potential  $\Phi$  can be used as the initial descriptive function. In practice, if we wish to determine all descriptive functions mentioned, the most convenient initial function is the spatial density  $\rho$ .

A large variety of analytic expressions has been proposed for the initial descriptive function. To select the most suitable expressions, the following conditions can be used (Kutuzov, Einasto 1968, Einasto 1969b, 1971):

- 1) the mass and luminosity densities must be always nonnegative and finite;
- 2) the mass density and its derivative must not have breaks, even at the centre of the system;
- 3) the density must decrease outwards;
- 4) the moments of the mass distribution function must be finite

$$M_j\{\mu\} = \int_0^{\infty} \mu(a) a^j da < \infty, \quad j \geq -2; \quad (11)$$

- 5) the descriptive functions are to form a mutually consistent system of functions;

6) the model of the galaxy must allow stable circular motions. It should be noted that in special types of galaxies some of these conditions may not be fulfilled.

A discussion of analytical expressions, used earlier in galactic models has shown (Einasto 1968a, b, 1969b) that almost all expressions do not satisfy some of the conditions mentioned. Therefore we have proposed a new density law (Einasto 1970b, Einasto and Einasto 1972a)

$$\rho(a) = \rho(0) \exp \left\{ x - [x^{2N} + a^2 (ka_0)^{-2}]^{1/2N} \right\}, \quad (12)$$

where

$$\rho(0) = h M (4\pi \epsilon a_0^3)^{-1} \quad (13)$$

is the central density of the component,  $M$  is the mass of the component,  $\alpha_e$  its effective (mean) radius, for definition of  $\alpha_e$  s. Einasto and Einasto (1972a),  $x$  and  $N$  are structural parameters,  $h$  and  $k$  dimensionless normalizing parameters, depending on  $x$  and  $N$ . Our experience has shown that by an appropriate choice of structural parameters the law (12) can be used in all cases.

The practical procedure of determining the model of a galaxy consists of three steps.

First, a photometric model of the galaxy is to be found. To determine a representative photometric model, the profiles of the galaxy in several photometric systems and both along major and minor axis are needed. The preliminary values of model parameters can be found from graphs by a comparison of the observed curves  $B$ ,  $B - V$ , and  $U - B$  versus  $\log A$  with theoretical ones. The final values of model parameters can be determined by a trial-and-error procedure, for this purpose special computation program is composed. In photometric models the following parameters can be found for the components of the galaxy: structural parameters, effective radii, axial ratios (flattenings), luminosities and colours. The colours give us the ratios of mass-to-luminosity ratios, for instance

$$B - V = (B - V)_{\odot} + 2.5 \log (f_B / f_V). \quad (14)$$

The second step is the determination of the mass distribution model. For this purpose absolute values of mass-to-luminosity ratios for all components are to be determined. For the central bright components they can be found from spectrophotometric data by the Spinrad's method, and independently by the virial theorem from velocity dispersion. For fainter components the absolute value of  $f$  can be estimated theoretically, on the basis of the results of calculations of the physical evolution of galaxies and their populations.

In the case of galaxies with composite structure the virial theorem has the form (Einasto 1971)



$$\langle \sigma_r^2 \rangle_k = \beta_r G \alpha_{ok}^{-1} \sum_{l=1}^n \mathcal{M}_l H_{kl} . \quad (15)$$

In this expression  $\langle \sigma_r^2 \rangle_k$  is the mean dispersion of radial velocities of the component  $k$  of the galaxy (this quantity can be determined from observations),

$$\beta_r = \beta_R \cos^2 i + \beta_z \sin^2 i , \quad (16)$$

where  $\beta_R$  , and  $\beta_z$  are coefficients, defined in Einasto and Einasto (1972a). Further,  $\alpha_{ok}$  is the mean radius of the component  $k$  ,  $\mathcal{M}_l$  - the mass of the component  $l$  and

$$H_{kl} = \int_0^{\infty} \mu_k^*(\alpha) m_l(\alpha) \alpha^{-1} d\alpha , \quad (17)$$

where  $\mu_k^*$  is the dimensionless mass distribution function of the component  $k$  ,  $\alpha = a/\alpha_{ok}$  , and

$$m_l(\alpha) = \mathcal{M}_l^{-1} \int_0^{\alpha} \mu_l(\alpha) d\alpha \quad (18)$$

is the dimensionless inner mass of the component  $l$  .

The final step in the construction of the model of the galaxy is the determination of its dynamical and kinematical descriptive functions. Knowing the mass distribution function, the gravitational potential of the whole galaxy and its gradients can be calculated. Thereafter the kinematical functions can be found for different components of the galaxy. The difficulty lies in the fact that the system of hydrodynamical equations is not closed: for the five functions  $\sigma_R$  ,  $\sigma_\theta$  ,  $\sigma_z$  ,  $V_\theta$  ,  $\gamma$  we have two equations (8), and (9) only.

An approximate solution can be obtained, supposing  $\gamma = 0$  and  $\sigma_R^2$  ,  $\sigma_\theta^2$  ,  $\sigma_z^2 \ll V_\theta^2$  . In this case we have from the first hydrodynamical equation for  $z = 0$

$$V_\theta^2 = RK_R \equiv V^2 , \quad (19)$$

where  $V$  is the circular velocity; and from the second equation (Jeans approximation)

$$\rho(z) \left( \sigma_z^2(z) \right)_0 = \int_x^{\infty} K_z(R, z) \rho(z) dz \quad (20)$$

The formulae (19) and (4) are the basic ones in the classical method of the determination of the models of oblate galaxies.

To obtain more accurate solution, three additional equations are to be used. Recently we proposed (Einasto 1970a) to close the system of equations by means of the formula (Kuzmin 1953)

$$y = Rz / (R^2 + z_0^2 - z^2), \quad (21)$$

the Lindblad formula

$$k_\theta = \sigma_\theta^2 / \sigma_R^2 = 1/2 (1 + \partial \ln V_\theta / \partial \ln R), \quad (22)$$

and the Kuzmin (1961) formula

$$k_z = \sigma_z^2 / \sigma_R^2 = k_\theta / (1 + k_\theta). \quad (23)$$

Formula (21) follows from the theory of the third integral of motion,  $z_0$  is a constant (in more general case  $z_0$  varies with  $R$  and  $z$ , s. Einasto and Rummel 1970). It should be noted that formulae (22) and (23) are valid near the plane of symmetry of a galaxy and for the flat components of a galaxy only. In the general case the problem of closing hydrodynamical equations is more complicated and has presently no final solution.

#### IV The Structure of galaxies

##### Populations in galaxies

The list of populations that can be separated at present in nearby external galaxies is given in Table 1.

In this list the term nucleus is preserved only for the massive non-stellar body in the centre of a galaxy responsible for its activity. The nature of galactic nuclei is not fully understood. According to Ozernoi and Usov (1971), for example, they are massive highly magnetized gaseous bodies. The masses

of galactic nuclei, given below, are estimated from the virial theorem.

The smallest stellar population in galaxies is called kernel, following a suggestion of Vorontsov-Velyaminov (1972). Earlier these objects have been also called galactic nuclei, but this may lead to a confusion with the non-stellar central bodies. The second new term, used here, is the core, defined as the central and the most metal-rich part of the bulge. The presence of this population in giant galaxies, which has almost the same metal abundance and mass-to-light ratio as the kernel, but much larger radius, is demonstrated by spectral (Spinrad et al. 1971) and photometric (Sandage et al. 1969) observations.

Both the bulge and the disc consist of stars of normal metal content. They differ by the mean age of stars (in the disc the age dispersion is much larger), flattening and the mean radius. Halo is characterized by a large deficit of metals. The young population consists of young stars and star generating medium (interstellar gas and dust), distributed irregularly or forming spiral arms.

Kernel, core, bulge and halo consist of old stars, which form in galaxies subsystems of nearly spherical form. In former classification no difference between these populations has been made, they have been called population II (Baade 1944) or spherical component (Kukarkin 1949). These populations differ by chemical composition, mean radii and densities.

In external galaxies we cannot observe individual stars belonging to transition populations between extreme halo and disc populations. But there exist indirect evidence that in external galaxies such transition populations do occur as it is the case with our Galaxy (long-period red variables, RR Lyrae stars with periods  $< 0.4$  days, moderately metal-deficit globular clusters). The mean axial ratio of equidensity ellipsoids, found from photometric data for the Andromeda galaxy, is  $\xi = 0.30$  for the halo and  $\xi = 0.08$  for the disc (Einasto 1971). Since extreme halo population objects (globular clusters) in M31 have  $\xi = 0.54$

(Einasto 1972a), there must exist intermediate subsystems with  $0.08 \leq \epsilon \leq 0.3$ . Kinematical data of stars in our Galaxy indicate that subsystems within this range of axial ratio  $\epsilon$  are associated with RR Lyrae stars of different mean periods. RR Lyrae stars belong to the metal deficient stars, therefore one may conclude that subsystems in this range of  $\epsilon$  are intermediate halo subsystems.

Young (extreme I (Oort 1958), flat (Kukarkin 1949)) population consists of subsystems, individual members of which are sufficiently bright for observations in the nearby galaxies (supergiant stars, stellar associations,  $H_\alpha$  -regions). The spatial structure of these subsystems is in general similar. However little differences exist, which play important role the developing of the theory of star formation.

#### Photometric models

Detailed models are now available for six galaxies: our Galaxy (Einasto 1970b, Einasto and Einasto 1972b), the Andromeda galaxy, M31 (Einasto 1971, Einasto and Rümmler 1972) and its dwarf elliptical companions, M32, the giant elliptical galaxy M87 and very faint dwarf elliptical galaxies in Fornax and Sculptor (present paper). The data on these galaxies are given in Tables 2 and 3. In Table 2 there are given: mass  $\mathcal{M}$ , blue luminosity  $L_B$ , effective radius  $a_0$ , axial ratio of equidensity surface  $\epsilon$ , mass-to-luminosity ratio  $f_B$ , two colours, B - V, U - B, mean density  $\langle \rho \rangle$ , defined by the expression

$$\langle \rho \rangle = \mathcal{M} (4\pi \epsilon a_0^3 \chi)^{-1}, \quad (24)$$

where  $\chi$  is a dimensionless constant of the order 1 (for definition of  $\chi$  see Einasto 1972b). Finally,  $B(0)$  is the central blue brightness of the component, seen face on and corrected for the effect of interstellar reddening, and  $P(0)$  is the central value of surface density (perpendicular to the plane of symmetry of the galaxy),  $N$  and  $x$  are structural parameters. In the Table 3 the adopted true distance modulus  $(m-M)_0$ , blue absorption

$$A_B = B - B_0, \quad \text{inclination angle } i, \quad \text{velocity dispersion}$$

in the centre  $\sigma_r$ , and spectrophotometrically determined mass-to-luminosity ratio  $f_V$  are given.

In Fig. 1 - 5 there are given photometric profiles along the major axis for all 5 galaxies studied. The curves represent components of galaxies and the total luminosity profiles, observations of various authors are plotted with different symbols. The agreement of models with observations is very good - the deviations are much smaller than the observational errors. The region of spiral arms in the Andromeda galaxy presents the only exception: the model does not represent individual spiral arms. In Fig. 6 - 7 the run of apparent axial ratio of equidensity ellipses is given for M87, and M31, in Fig. 8 - the colour variation for M87. As seen, these photometric functions are also satisfactorily reproduced by the model.

#### Mass-to-luminosity ratio of components

The critical point in model constructing is the determination of mass-to-luminosity ratios for individual galactic components.

For the kernel and the core this ratio can be determined from observations by two methods, namely from spectrophotometric data and from the virial theorem. The necessary observational data are given in Table 3. Both kind of data are available for M31 and M32 and give mutually consistent results. The adopted values for  $f_B$  are given in Table 2.

For the other extreme case, the halo, we have no direct determinations of  $f_B$ . From the analogy with globular clusters we may assume that  $f_B$  is approximately equal to 1 (Schwarzschild and Bernstein 1955). This value represents, however, a low limit for the halo, since the low mass stars with high values of  $f_B$  may evaporate from clusters, what is not the case with halos. We have adopted a preliminary value  $f_B = 3$  for the halos of all galaxies considered. There may exist differences in  $f_B$  for the halos of galaxies of different mass and morphological type, but more information is needed to make quantitative conclusions.

The mass-to-luminosity ratio of the young population is estimated from theoretical calculations of the physical evolution of galaxies (Einasto 1974). The mass of interstellar gas is also included into the mass of this component.

For the bulge and the disc the mass-to-luminosity ratio can be found from the total mass of the galaxy, known from rotation velocity data (M31), and from physical evolution calculations. We assume that in M31 the bulge and the disc have the same chemical composition and that mass-to-luminosity ratio differences are caused by differences in age distribution of stars. The latter can be estimated by physical evolution calculations. The absolute values of  $f_B$  are found from the total mass of M31 (the masses of all other components are calculated from luminosities and mass-to-luminosity ratios).

For M87 and M32  $f_B$  of the bulge can be estimated from physical evolution calculations. These estimates are however rather rough, since the chemical composition is known approximately only. A better estimate can be found from  $B-V$ ,  $U-B$  colours, by means of the correlation between integrated colours and mass-to-luminosity ratios for the old populations.

The dependence of  $\log f_B$  of individual galactic components on the total mass of the galaxy  $M$  and on the  $B-V$  and  $U-B$  colours is shown in Fig. 9 and 10. We see that a close correlation exists between these quantities. Since all populations plotted in Fig. 9 and 10 have approximately the same age, the differences in  $f_B$  can be attributed to differences in composition.

#### Mass, mass-to-luminosity, and circular velocity distribution

For all galaxies studied the general mass, mass-to-luminosity and circular velocity distribution have been calculated. The general mass distribution has been found from the formula

$$M(\alpha) = \sum_{j=1}^n \int_0^{\alpha} \mu_j(\alpha) d\alpha, \quad (25)$$

where  $n$  is the number of components in the particular galaxy.

The general mass-to-luminosity ratio has been calculated from the expression

$$f_B(\alpha) = P(\alpha)/L_B(\alpha) , \quad (26)$$

where  $P(\alpha)$  and  $L_B(\alpha)$  are the face-on projected mass and luminosity densities (summed over all components), projected luminosity being corrected for the interstellar absorption.

In Fig. 11 the general mass distribution is plotted for 5 galaxies, the lines of constant mean inner densities

$$\langle \rho(\alpha) \rangle = 3 M(\alpha) (4\pi\alpha^3)^{-1} \quad (27)$$

are also given. These densities correspond to the spherical distribution of mass. In Fig. 12 the run of the mass-to-luminosity ratio is given for the same 5 galaxies. In Fig. 13 the circular velocity curve is given for the Andromeda galaxy, M31. For the sake of comparison the corresponding functions are given for the Andromeda galaxy according to the Roberts (1966) model, a typical representative of models, constructed by the classical method.

Let us compare Roberts model with the new one.

The main difference between the old and new models lies in the mass concentration to the centre. The new model has a very high mass concentration: 25 % of the total mass is located inside a spheroid with major-semiaxis  $a = 1.8$  kpc, the corresponding mean inner density is  $\langle \rho(\alpha) \rangle = 2 M_{\odot} \text{pc}^{-3}$ . In the Roberts model 25 % of the total mass is located inside the spheroid  $\alpha = 9$  kpc with mean density  $\langle \rho(\alpha) \rangle = 0.03 M_{\odot} \text{pc}^{-3}$ . The central densities differ drastically:  $\rho(0) = 10^6 M_{\odot} \text{pc}^{-3}$  in the new model, and  $\rho(0) = 1.4 M_{\odot} \text{pc}^{-3}$  in Roberts's model. Since the luminosity density increases rapidly to the centre, the mass-to-luminosity ratio in old models decreases to the centre (Fig. 12). In the centre according to Roberts's model  $f_B(0) = 10^{-2}$ .

Main arguments against old models of spiral galaxies can be summarized as follows.

1. Direct density estimates, based on the virial theorem, give

for the central region values of 5 to 6 orders of magnitudes greater than follows from old models.

2. Direct mass-to-luminosity ratio determinations based on spectrophotometric observations gives for the centres of spiral galaxies values, 3.5 orders of magnitude greater than those following from old models.

3. It is impossible to obtain theoretically a mass-to-luminosity ratio decreasing toward the centre, for physically reasonable values of parameters of star formation function.

4. The physical characteristics of central regions of spiral galaxies are very similar to the corresponding characteristics of elliptical galaxies, therefore it is highly improbable that the run of mass-to-luminosity ratio in the central regions of these galaxies is fully different.

5. Since the velocity dispersion in the central parts of galaxies is large (determined spectroscopically and confirmed by model calculations), the rotational velocity must be much smaller than the circular one. For the kernel of M31 the observed angular rotational velocity amounts to 7 % of the angular velocity of circular motion only (Einasto 1972a).

#### The problem of "missing mass" in galaxies

Oort (1960) and Hill (1960) have investigated vertical motions of stars in the solar vicinity and determined the vertical gradient of the gravitational acceleration, characterized by the Kuzmin parameter  $C$ ,

$$C^2 = -(\partial K_z / \partial z)_{z=0} . \quad (28)$$

By means of the Poisson equation (Kuzmin 1952)

$$4\pi G \rho = C^2 - 2(A^2 - B^2), \quad (29)$$

where  $A$  and  $B$  are Oort constants, the total dynamical density of matter  $\rho$  in the solar vicinity has been calculated. The result



is  $C = 90 \text{ km sec}^{-1} \text{ kpc}^{-1}$  and  $\rho = 0.150 M_{\odot} \text{ pc}^{-3}$ , about twice the observed star and interstellar gas density  $\rho = 0.091 M_{\odot} \text{ pc}^{-3}$  (Einasto and Kutuzov 1964). The difference has been attributed to stars of unknown origin. Hence the problem of "missing mass" arises.

Kuzmin (1955), Belsalu (1958) and Einasto (1966) have found a considerable smaller value  $C = 70 \text{ km sec}^{-1} \text{ kpc}^{-1}$  in good agreement with direct estimates of mass density. Recently Jõeveer (1972) developed a new method for the determination of  $C$ . The result is again  $C = 70 \text{ km sec}^{-1} \text{ kpc}^{-1}$ . Therefore the hypothesis of the presence of unknown matter in the solar vicinity in a great amount seems to have no strong observational support.

This problem has arisen however newly in connection with a different phenomenon. Calculated circular velocities possess a considerably steeper radial gradient at the outer regions of spiral galaxies as follows from observations of rotational velocities. That can be seen in Fig. 13 from a comparison of our model with the Roberts's one - the latter reproduces direct observations fairly well. These differences may be explained in two ways.

1. In the outer regions of spiral galaxies there exist large systematical deviations of rotational velocities from circular ones.

2. Spiral galaxies have coronas of great masses and dimensions.

The first hypothesis is supported by the discovery of Roberts (1967) and Courtes et al. (1968) that many spiral galaxies have large differences in rotation curves of opposite sides, which can hardly attribute to differences in circular velocities.

If the second hypothesis is correct, the discrepancy between the total cosmological density of matter and the mean density of observed matter (Shapiro 1971) would become less drastical. The matter considered can not be in the form of neutral gas, since this gas would be observable. Luminosity decreases in outer galactic regions rapidly, therefore, if the matter is in the form of stars, the latter must be of very low luminosity. The presence of low luminosity stars in outer galactic regions without bright

ones would require a powerful process of large-scale segregation of stars according to the mass (low luminosity stars have smallest masses), but this is highly improbable. There remains the possibility that the unknown matter exists in the form of rarefied ionized gas. If this is the case, it would perhaps explain the discrepancy between the virial and count masses of clusters of galaxies. The corona is added in our model B, its mass is estimated to be equal to the stellar component of the galaxy ( $185 \times 10^9 M_{\odot}$ ), the effective radius  $\alpha_0 = 20$  kpc, and the mean density about  $10^{-3} M_{\odot} \text{pc}^{-3}$ .

There exist some evidence that very massive gaseous coronae may surround giant elliptical galaxies too. If we suppose that outer limiting radii of galaxies, containing practically all their masses, do not change with time and that the corresponding mean densities characterize the initial densities of protogalaxies at the time of galaxy formation, we obtain for the initial density of M87  $3 \cdot 10^{-5} M_{\odot} \text{pc}^{-3}$ , what is about 1.5 orders of magnitude smaller than the initial density of M31,  $10^{-3} M_{\odot} \text{pc}^{-3}$ . The initial densities of both galaxies would be equal if the galaxy M87 has a corona of the mass  $2 \cdot 10^{13} M_{\odot}$  and of the effective radius  $\alpha_0 = 100$  kpc (model B). We see that the total mass of the corona may be one order of magnitude greater than the mass of stellar component of the galaxy! In connection with this we refer to the recent investigation of De Young (1972), who has given evidence for the presence of intergalactic medium in clusters of galaxies.

The evidence of the presence of massive coronae around giant galaxies is however not very strong and further studies are necessary.

#### V Stellar orbits and kinematical properties of galactic populations

The knowledge of stellar orbits in galaxies is important in several respects. To establish the possible existence and form of the third integral of motion it is necessary to compute three-

dimensional orbits of stars. To develop the theory of evolution of stars the places of star formation must be known, which can be found by backward orbit calculations. The statistics of orbital elements is needed both for the theory of galaxy evolution and for the constructing of representative models of galaxies.

### Stellar orbits and the third integral of motion

According to the Jeans theorem (Jeans 1915) the phase density of stars depends on velocity components  $v_R$ ,  $v_\theta$ ,  $v_z$  through isolating integrals of motion  $I_i$ . In the case of steady state stellar systems, symmetrical in respect to a plane and axis of rotation, there exist in general two independent isolating integrals of motion - the energy integral  $I_1$  and the angular momentum integral  $I_2$ . If there exist no more isolating integrals the star density in the velocity space is a function of  $I_1$  and  $I_2$  only, and the velocity distribution is axially symmetrical, dispersions  $\sigma_R$  and  $\sigma_z$  being equal. This contradicts observations: in the solar vicinity the dispersion of radial motions for all subsystems of stars studied exceeds the dispersion of vertical motions.

This discrepancy has sometimes been interpreted as an indication of the non steady state of the Galaxy. However Kuzmin (1953) has pointed out that the inequality of the velocity dispersions can be explained in the framework of the theory of stationary galaxy, provided we suppose the existence of third isolating integral of motion,  $I_3$ . As a first approximation, a quadratic dependence of  $I_3$  on velocity components has been supposed. The existence of a third quadratic integral of motion impose definite restriction for the gravitational potential of the galaxy. The corresponding form of potential has been proposed already by Eddington (1915). Kuzmin (1953, 1956) has shown that this form of potential enables us to construct reasonable models of galaxies.

In the case of the quadratic third integral the galactic orbits of stars are located inside of toroids bordered by confocal hyperboloids and ellipsoids. Two projections of such an orbit, calculated in 1953 by Eelsalu are given in Fig. 14. Later these

orbits have been called box-orbits (Ollongren 1962).

The family of confocal hyperboloids and ellipsoids has another important property. Together with the meridional planes they are tangent to the axes of velocity ellipsoids, and are therefore called the main velocity surfaces (Eddington 1915).

The gravitational potential of real galaxies does not exactly coincide with the potential following from the theory of the quadratic third integral. Therefore, if the third isolating integral exists, it does not have a quadratic form and the main velocity surfaces are not confocal hyperboloids and ellipsoids. To verify the possible existence of the third integral Ollongren (1962) has computed a series of three-dimensional orbits of stars for the Schmidt (1956) model of the Galaxy. As in the previous case the orbits are located in toroids, but they have a more complicated form of meridional sections. This seems to show that the third isolating integral exists, but does not have a quadratic form.

Recent studies, reported in IAU Symposium No. 25 (Contopoulos 1966), indicate that the problem is more complicated, however. For some regions of the galaxy meridional sections of stellar orbits are enveloped by boxes, indicating the isolating character of the third integral. In other regions stellar orbits fill all the space allowed by the energy integral, in this region the third integral is not isolating (ergodic orbits).

From the standpoint of galaxy modelling one important problem to be solved is the determination of the tilt  $\alpha(R, z)$  of the velocity ellipsoid outside the equatorial plane. This problem is solved so far only for the case, when the third integral has a quadratic form and the main velocity surfaces are confocal hyperboloids and ellipsoids.

#### Stellar orbits and places of star formation

The possibility of backward orbit calculations and the knowledge of stellar ages enables us to find the places of star formation. For this purpose Contopoulos and Strömgren (1965) have published extensive tables of plane galactic orbits. Recently

Grossman and Yuan (1970) calculated new tables of plane galactic orbits for potential with spiral component.

Orbit calculations have been used for the derivation of places of star formation by Dixon (1967a, 1967b, 1968). He has found that stars do form near the apocentra its orbits and then fall toward the centre of the galaxy. According to a suggestion of Oort (1964), the reason for this is that interstellar gas is supported partly by non-gravitational forces. This problem has been studied also by Hube (1970) who has found no clustering of star formation points near apocentra.

Vertical oscillations of stars have been studied also by Jõe-veer (1968, 1972). He has shown that groups of young stars do oscillate synchronously with the frequency  $\omega_z = C = 70 \text{ km sec}^{-1} \text{ kpc}^{-1}$ . This is the case if stars do form above or below the galactic plane with small random velocities, as suggested by Oort. Hube has failed to prove the existence of such vertical oscillations since he has adopted too large value  $C = 90 \text{ km sec}^{-1} \text{ kpc}^{-1}$  for the Kuzmin constant.

#### Statistics of stellar orbits and kinematical properties of galactic populations

Statistics of the elements of stellar orbits, as well as velocity dispersions and centroid velocities yield valuable information on kinematical properties of galactic populations. In our Galaxy kinematical characteristics can be determined for solar vicinity for all populations of stars, but the parameters of spatial distribution only for subsystems of bright stars. This makes kinematical characteristics very useful for the determination of the mean age of a given star groups.

For cosmogonic studies both the statistics of stellar orbital elements and the statistics of velocity components can be used.

The first procedure has been used by Eggen, Lynden-Bell and Sandage (1962) to study the initial collapse phase of the Galaxy history. Individual orbits of large number of stars have been calculated and then orbital elements found. The same results

could be obtained more directly from the three-dimensional Bottlinger diagram, that gives the orbital elements directly from the components of velocity vectors of stars (Kuzmin 1956).

Centroid velocities and elements of velocity dispersion tensor have been used for the study of galactic dynamical evolution by von Hörner (1960) and Einasto (1970b, 1971). In both studies absolute ages have been found for some subsystems, that allows to accomplish age calibration for all kinematic groups. All these studies showed that at the first phase of its evolution the Galaxy was rapidly contracting both in radial and vertical directions.

If the mass density and gravitational potential of a galaxy is known, it is possible to calculate kinematical descriptive functions for various test-populations by means of formulae given in section III. Such calculations have been carried out for seven test-populations of our Galaxy and six test-populations of the Andromeda galaxy (Einasto 1971). The results for one test-population of our Galaxy are given in the Fig. 15. In addition to kinematical functions the density of the population and its gradients are also plotted,

As mentioned in section III, one important kinematical parameter is the ratio of velocity dispersions  $k_z$ . The Kuzmin formula (23) gives for the solar vicinity  $k_z = 0.285$  in good agreement with observed value for flat subsystems,  $k_z = 0.278$ . For intermediate and halo subsystems the direct determination of  $k_z$  is difficult due to large observational errors. This quantity can be determined, however, indirectly by integration of the hydrodynamical equations (8) and (9), adopting the observed relation between the centroid velocity and the mean velocity dispersion. The resulting dependence of  $k_z$  on the flattening of test-populations is reproduced in Fig. 16 (Einasto 1971).

## VI The evolution of galaxies

Now we consider the application of the method of modelling to the study of the evolution of galaxies.

The evolution of galaxies is caused by four different processes: the formation of stars out of interstellar matter, the

enrichment of the interstellar matter by the products of stellar evolution, the change of physical parameters of populations as a result of stellar evolution, and the change of spatial distribution of stars and interstellar matter. All processes are working simultaneously and are mutually affecting one another. For instance, the rate of star formation depends on the density of interstellar matter, the contraction of interstellar matter is controlled by the number of young hot stars etc. Therefore a perfect theory of galaxy evolution must take into account all processes simultaneously. However, the problem is very complicated and such a theory does not exist at present. A separate study of different processes seems to be a realistic approach.

To construct models of physical evolution of galaxies the following data are needed: the rate of star formation as a function of time, the distribution of newly-born stars according to their mass (the initial mass function), the evolution tracks of stars of different masses and composition, the rate of production of various isotopes by stars of different mass, and the bolometric corrections and intrinsic colours of stars as functions of their chemical composition, absolute temperature and luminosity. The latter data are necessary to calculate observable photometric quantities for model galaxies.

Dynamical parameters of stellar populations are rather conservative, therefore the present dynamical state of the populations preserve information on the conditions in the galaxy at the time of their formation. Comparing the dynamical parameters of populations of different ages, it is possible to reconstruct the past dynamical history of the galaxy.

#### The rate of star formation

Oort (1958) supposed that the rate of star formation is proportional to the interstellar gas density in a rather high power. This was confirmed by Schmidt (1959) who found from the study of star and gas densities in the solar vicinity that

$$R \equiv d\varphi_s/dt = \gamma \varphi_g^n . \quad (30)$$

For the power of this empirical law Schmidt obtained the value  $n = 2$ . Practically the same result  $n = 1.84$  has been found by Sanduleak (1969) for Small Magellanic Cloud. Recently Hartwick (1971) has found for the Andromeda galaxy, M31, a considerable higher value,  $n = 3.5$ , and has supposed that this parameter may depend on local conditions of star formation. However, Hartwick has used hydrogen densities, uncorrected for the antenna smearing effect. A rediscussion of the data on M31, the antenna smearing effect taken into consideration, gives  $n = 2$  (Einasto 1972b). In the last-mentioned study the coefficient of proportionality,  $\gamma$ , has also been found. A value  $\gamma = 4$  has been obtained (time being expressed in  $10^9$  years and densities in solar masses per cubic parsec). The result corresponds to normal chemical composition of the gas. The available data indicate that at very low gas densities ( $\varphi_g < 0.01 M_{\odot} \text{pc}^3$ ) star formation does not take place.

Of course, the rate of star formation depends not only on the gas density. It depends also on the temperature and composition of the gas, may be on other factors too. An attempt to take into account the temperature and the composition of the gas has been made by Matsuda (1970). The adopted dependence is however rather arbitrary.

If the total density of matter  $\rho = \rho_s + \rho_g$  is supposed to be independent of time, the differential equation (30) can be integrated analytically. The result for the mass of gas  $M_g$  in the galaxy is in case  $n = 2$ :

$$M_g = M (1 + \tau)^{-1} , \quad (31)$$

where  $M$  is the total mass of the galaxy,

$$\tau = t/t_0 \quad (32)$$

the dimensionless time, and

$$t_0 = (\gamma \langle \varphi \rangle)^{-1} \quad (33)$$



the characteristic time of star formation,  $\langle \rho \rangle$  being the mean total density of matter in the galaxy. It should be mentioned that the widely used exponential law (Tinsley 1968)

$$M_g = M e^{-\tau} \quad (34)$$

corresponds to the case  $n = 1$  and contradicts the Schmidt law.

The initial luminosity function has been derived first by Salpeter (1955), who found that the distribution of the number of newly born stars according to their masses  $m$  can be satisfactorily expressed by the law

$$F(m) = \alpha m^{-p}, \quad (35)$$

$\alpha$  being a normalizing constant and  $p = 2.35$ . This law has been confirmed by Sandage (1957), van den Bergh (1957) and others. Reddish (1965) turned attention to the case  $p = 2.33$  that corresponds to the equal distribution of the potential energy among stars of different mass. Saar (1972) has shown that this particular case is valid in a very wide range of masses of celestial bodies from stars to clusters of galaxies. The law (35) cannot be applied to very small masses as the integral  $\int F(m) dm$  do not converge. Therefore an effective lower limiting mass  $m_0$  must exist.

Models of physical evolution of galaxies have been constructed by Tinsley (1968) and Einasto (1971), using evolutionary tracks of stars, bolometric corrections, and intrinsic colours. The main results of these studies are the following.

Tinsley has made an attempt to reproduce the observed integrated photometric properties of galaxies by a corresponding choice of parameters of the stellar birth function. Chemical composition of stars has not been varied. In this case the necessary variations of other parameters become too large. In particular, the observed high values of mass-to-luminosity ratios of giant elliptical galaxies have been achieved by adding arbitrarily red dwarfs in an unprobable large amount.

Our study has shown that the most important factor in galactic evolution is the initial chemical composition of stars. In Fig. 17 we reproduce the dependence of  $f_B$  on time for three different compositions. Following a suggestion of Truran and Cameron (1970) we suppose that the lower limiting mass of stellar birth function depends on the composition of the gas. For the normal composition  $Z = 0.02$  we adopt (Reddish 1965)  $m_o = 0.03 M_\odot$ , for  $Z = 0.10$   $m_o = 0.001 M_\odot$  and for  $Z = 10^{-5}$   $m_o = 0.1 M_\odot$ .

The other important parameter, determining the evolution of galaxies, is the mean density. Differences in mean density may be responsible for the formation of galaxies of different types: ellipticals, spirals and irregulars (Holmberg 1964). However serious difficulties arise if we wish to explain the formation of different populations by differences in their mean density alone.

The characteristic times of star formation  $t_o$ , calculated for various components of galaxies (Table 2) vary in very broad limits. In particular, the characteristic time for the formation of the halo is too large. To overcome this difficulty one may suppose that the parameter  $\gamma$  of the Schmidt law (30) is not constant, but depends on the chemical composition of interstellar gas. This assumption cannot explain, however, the presence of halos of different mean densities, since the halo stars in different galaxies have approximately the same composition. There remains another explanation - to suppose that halo stars are formed at the final stage of the contraction of the protogalaxy just before gas clouds have lost their high kinetic energy by collisions. Otherwise we suppose that halo stars are formed near the pericentra of their first revolution. At that time the mean density of the protogalaxy was high and a fast formation of halo stars was possible.

#### Dynamical evolution of galaxies

The differences in kinematical properties and corresponding parameters of spatial distribution of stars of different spectral types have been known long ago (Rootsmäe 1943, Kukarkin 1949, Parenago 1951). Rootsmäe has interpreted these data as an age effect.

He supposed that the star generating medium (gas) was in a gradual contraction. A different explanation has been proposed by Spitzer and Schwarzschild (1953), Gurevitch (1954) and Kuzmin (1961): the acceleration of stars by interaction with massive clouds of interstellar matter and stars (the effect of irregular gravitational forces).

Von Hörner (1960) showed that both processes are active in galaxies. In the initial phase of the galactic history the first process (rapid contraction of interstellar matter to the centre and plane of the galaxy) is dominating, thereafter the second process (acceleration) takes over. The contraction or collapse phase has been studied in detail by Eggen, Lynden-Bell and Sandage (1962) and recently by Einasto (1971). Von Hörner results have been confirmed. In central parts of the Galaxy the contraction proceeds very quickly (in  $10^7$  years), the bulge and inner halo are formed in few  $10^8$  years, the formation of the disc is completed within  $10^9$  years. The degree of contraction of the gas is very large in the centre of the galaxy (about 100), in the solar vicinity the degree of radial contraction of the gas is about 5, and the degree of vertical contraction - about 50 (Fig. 18).

The consequences of fast initial contraction of the galaxy have been investigated by Lynden-Bell (1967b). He showed that as the result of a fast change of the gravitational field violent relaxation takes place. This relaxation explains the similarity of density distribution of all elliptical galaxies. Recent numerical studies have confirmed these results (s. Contopoulos 1970).

The role of angular momentum of the protogalaxy to its subsequent evolution is also to be mentioned. This problem has been investigated by many authors (Lynden-Bell 1967a, Brosche 1970, Sandage et al. 1970). The protogalaxies with small relative angular momentum lead to the formation of elliptical galaxies, the protogalaxies with large momentum - to the formation of spiral and irregular galaxies.

It is usually adopted that the angular momentum distribution

in galaxies is identical to the corresponding distribution of a uniformly rotating homogeneous spheroid (Crampin and Hoyle 1964, Innanen 1966). This result is based, however, on old models of spiral galaxies, where the central mass concentration is underestimated. The only spiral galaxy, for which a new model is available, is the Andromeda galaxy. The angular momentum distribution of M31 is reproduced in Fig. 19 (Einasto 1971). We see that there exists a large excess of mass of low momentum as compared with the homogeneous spheroidal model. This result shows that the main conclusion of Crampin and Hoyle, that the Galaxy has condensed from a homogeneous spheroid without turbulent mixing, may be incorrect.

#### References

- Arp, H. and Bertola, F.: 1969, *Astroph. Lett.* 4, 23.  
 Baade, W.: 1944, *Astrophys. J.* 100, 137.  
 Baade, W. and Arp, H.: 1964, *Astrophys. J.* 139, 1027.  
 Bergh, S. van den: 1957, *Astrophys. J.* 125, 445.  
 Bergh, S. van den: 1964, *Astrophys. J. Suppl.* 9, 65.  
 Bergh, S. van den: 1967, *Astron. J.* 72, 70.  
 Bergh, S. van den: 1968, *David Dunlap Obs. Comm. No.* 195.  
 Bergh, S. van den: 1969, *Astrophys. J. Suppl.* 19, 145.  
 Brandt, J.C. and Roosen, R.G.: 1969, *Astrophys. J. (Lett.)* 156, L59.  
 Brosche, P.: 1970, *Astron. Astrophys.* 6, 240.  
 Contopoulos, G. (ed.): 1966, *The Theory of Orbits in the Solar System and in Stellar Systems*, IAU Symposium No.25, Acad. Press, N.Y.  
 Contopoulos, G.: 1970, *Thessaloniki Contr. No.* 53.  
 Contopoulos, G. and Strömberg, B.: 1965, *Tables of Plane Galactic Orbits*, Inst. Space Studies, N.Y.  
 Courtes, G., Garranza, G., Georgelin, Y., Monnet, G., Pourcelot, A.: 1968, *Ann. Astrophys.* 31, 63.  
 Crampin, D.J. and Hoyle, F.: 1964, *Astrophys. J.* 140, 99.  
 Deharveng, J.M. and Pellet, A.: 1969, *Astron. Astrophys.* 1, 208.  
 De Young, D.S.: 1972, *Astrophys. J. (Lett.)* 173, L7.  
 Dixon, M.E.: 1967a, *Monthly Notices Roy. Astron. Soc.* 137, 337.  
 Dixon, M.E.: 1967b, *Astron. J.* 72, 429.

- Dixon, M.E.: 1968, Monthly Notices Roy. Astron. Soc. 140, 287.
- Eddington, A.S.: 1915, Monthly Notices Roy. Astron. Soc. 76, 37.
- Belsalu, H.: 1958, Publ. Tartu Astron. Obs. 33, 153.
- Eggen, O.J., Lynden-Bell, D. and Sandage, A.R.: 1962, Astrophys. J. 136, 748.
- Einasto, J.: 1966, Transact. IAU XIIB, 436.
- Einasto, J.: 1968a, Publ. Tartu Astron. Obs. 36, 396.
- Einasto, J.: 1968b, Publ. Tartu Astron. Obs. 36, 414.
- Einasto, J.: 1969a, Astrofiz. 5, 137.
- Einasto, J.: 1969b, Astron. Nachr. 291, 97.
- Einasto, J.: 1970a, Astrofiz. 6, 149.
- Einasto, J.: 1970b, Tartu astr. obs. Teated No. 26, 1.
- Einasto, J.: 1971, Structure and Evolution of Regular Galaxies, Tartu (unpublished).
- Einasto, J.: 1972a, in External Galaxies and Quasi Stellar Objects, ed. D.S.Evans, Reidel, Dordrecht, p. 37.
- Einasto, J.: 1972b, Astrophys. Lett. 11, 195.
- Einasto, J. and Einasto, L.: 1972a, Tartu astr. obs. Teated No. 36, 3.
- Einasto, J. and Einasto, L.: 1972b, Tartu astr. obs. Teated No. 36, 46.
- Einasto, J. and Kutuzov, S.A.: 1964, Tartu astr. obs. Teated No. 10, 1.
- Einasto, J. and Rümmler, U.: 1970, Astrofiz. 6, 241.
- Einasto, J. and Rümmler, U.: 1972, Tartu astr. obs Teated No. 36, 55.
- Grossman, K. and Yuan, C.: 1970, Tables of Plane Galactic Orbits with Spiral Field, Inst. Space Studies.
- Gurevitč, L.E.: 1954, Voprosy Kosmogoni 2, 151.
- Hartwick, F.D.A.: 1971, Astrophys. J. 163, 431.
- Hill, E.R.: 1960, Bull. Astron. Inst. Netherl. 15, 1.
- Hodge, P.W.: 1961a, Astron. J. 66, 249.
- Hodge, P.W.: 1961b, Astron. J. 66, 384.
- Holmberg, E.: 1964, Uppsala Astr. Obs. Medd. 148.
- Hörner, S. von: 1960, Mitt. Astr. Rechen-Inst. Heidelberg, Ser. A, 13.
- Hube, D.P.: 1970, Astron. Astrophys. 9, 142.
- Innanen, K.A.: 1966, Astrophys. J. 143, 150.
- Jéans, J.H.: 1915, Monthly Notices Roy. Astron. Soc. 76, 70.
- Jõeveer, M.: 1968, Publ. Tartu Astron. Obs. 36, 84.
- Jõeveer, M.: 1972, Tartu astr. obs. Teated, No. 37, 3.
- Johnson, H.M.: 1961, Astrophys. J. 133, 309.

- King, I.R.: 1971, Publ. astr. Soc. Pacific 83, 377.
- Kinman, T.D.: 1963, Astrophys. J. 137, 213.
- Kukarkin, B.V.: 1949, The Investigation of the Structure and Evolution of Stellar Systems on the Basis of the Study of Variable Stars, Gostechizdat, Moscow.
- Kuzmin, G.G.: 1952, Publ. Tartu Astron. Obs. 32, 5.
- Kuzmin, G.G.: 1953, Publ. Tartu Astron. Obs. 32, 332.
- Kuzmin, G.G.: 1955, Publ. Tartu Astron. Obs. 33, 3.
- Kuzmin, G.G.: 1956, Astr. Zu. 33, 27.
- Kuzmin, G.G.: 1961, Publ. Tartu Astron. Obs. 33, 351.
- Kuzmin, G.: 1969, Astronomy and Geodesy in Estonian SSR, Tartu , p.52.
- Kutuzov, S.A. and Einasto , J.: 1968, Publ. Tartu Astron. Obs. 36, 341.
- Liller, M.H.: 1960, Astrophys. J. 132, 306.
- Lynden-Bell, D.: 1967a, Radio Astronomy and the Galactic System, ed. H. van Woerden, Acad. Press, N.Y. , p. 257.
- Lynden-Bell, D.: 1967b, Monthly Notices Roy. Astron. Soc. 136, 101.
- Matsuda, T.: 1970, Progr. Theor. Phys. 43, 1491.
- Mc Clure, R.D.: 1969, Astr. J. 74, 50.
- Minkowsky, R.: 1962, Problems of Extra-Galactic Research, ed. G.G.McVittie, MacMillan , N.Y. , p. 112.
- Morgan, W.W. and Mayall, N.U.: 1957, Publ. astr. Soc. Pacific 69, 291.
- Ollongren, A.: 1962, Bull. Astron. Inst. Netherl. 521, 241 .
- Oort, J.H.: 1958, Ric. astr. Specola astr. Vatic. 5, 415.
- Oort, J.H.: 1960, Bull. Astron. Inst. Netherl. 15, 45.
- Oort, J.H.: 1964, The Galaxy and the Magellanic Clouds, eds. F.J. Kerr, A.W.Rodgers, Canberra, p.1.
- Ozernoy, L.M. and Usov, V.V.: 1971, Astrophys. Space Sci. 13, 3.
- Parento, P.P.: 1951, Trudy gos. astr. Inst. Sternberga 20, 26.
- Perek, L.: 1962, Adv. Astron. Astrophys. 1, 165.
- Racine, R.: 1968, J. Roy. Astr. Soc. Canada 62, 367.
- Reddish, V.C.: 1965, Vistas in Astronomy 7, 173.
- Richter, N. and Högnér, W.: 1963, Astr. Nachr. 287, 261.
- Roberts, M.S.: 1966, Astrophys. J. 144, 639.
- Roberts, M.S.: 1967, Oral presentation to the IAU Commission 33 Meeting, Prague.
- Rootsmäe, T.: 1943, Tartu astr. obs. Kalender 74.

- Saar, E.: 1972 (personal communication).
- Salpeter, E.E.: 1955, *Astrophys. J.* 121, 161.
- Sandage, A.: 1957, *Astrophys. J.* 125, 422.
- Sandage, A.: 1968, *Astrophys. J. (Lett.)* 152, L149.
- Sandage, A.R., Becklin, E. and Neugebauer, G.: 1969, *Astrophys. J.* 157, 55.
- Sandage, A., Freeman, K.C. and Stokes, N.R.: 1970, *Astrophys. J.* 160, 831.
- Sanduleak, N.: 1969, *Astr. J.* 74, 47.
- Schmidt, M.: 1956, *Bull. Astron. Inst. Netherl.* 13, 15.
- Schmidt, M.: 1959, *Astrophys. J.* 129, 243.
- Schwarzschild, M. and Bernstein, S.: 1955, *Astrophys. J.* 112, 200.
- Shapiro, S.L.: 1971, *Astr. J.* 76, 291.
- Sharov, A.S.: 1963, *Astron. Zu.* 40, 900.
- Sharov, A.S.: 1968a, *Astron. Zu.* 45, 146.
- Sharov, A.S.: 1968b, *Astron. Zu.* 45, 335.
- Spinrad, H.: 1962, *Astrophys. J.* 135, 715.
- Spinrad, H.: 1971, *Pont. Acad. Scient. Scripta Var.* 35, 45.
- Spinrad, H., Greenstein, J.L., Taylor, B.J. and King I.R.: 1970, *Astrophys. J.* 162, 891.
- Spinrad, H., Gunn, J.E., Taylor, B.J., Mc Clure, R.D. and Young, J.W.: 1971, *Astrophys. J.* 164, 11.
- Spinrad, H. and Taylor, B.J.: 1971a, *Astrophys. J.* 163, 303.
- Spinrad, H. and Taylor, B.J.: 1971b, *Comments on Astroph. and Space Physics* 3, 40.
- Spitzer, L. and Schwarzschild, M.: 1953, *Astrophys. J.* 118, 106.
- Tammann, G.A.: 1970, *Astron. Astrophys.* 8, 458.
- Tinsley, B.M.: 1968, *Astrophys. J.* 151, 547.
- Truran, J.W. and Cameron, A.G.W.: 1970, *Nature* 225, 710.
- Vaucouleurs, G.de: 1953, *Monthly Notices Roy. Astron. Soc.* 113, 2.
- Vaucouleurs, G.de: 1958, *Astrophys. J.* 128, 465.
- Vaucouleurs, G. de: 1969, *Astrophys. Letters* 4, 17.
- Vaucouleurs, G.de and Ables, H.D.: 1968, *Mc Donald Observatory of the University of Texas* 414.
- Westerlind, B.E. and Wall, J.V.: 1969, *Astr. J.* 74, 335.
- Vetešnik, M.: 1962, *Bull. astr. Inst, Csl.* 13, 180.
- Woerden, H. van: 1967, *IAU Symp. No.* 31.
- Vorontsov-Velyaminov, B.A.: 1972, *Extragalactic astronomy*, Nauka, Moscow.

Table 1

## Galactic Populations

Population	$\epsilon$	$-\log Z$	$\log \frac{a_0}{a_{0, \text{halo}}}$	$\log t$ years
Kernel	1	1	-3	10
Core	1	1	-1.5	10
Bulge	1	1.5	-0.5	10
Halo	0.1 - 1	2 - 5	0	10
Disc	0.04 - 0.1	1.5	0.5	9 - 10
Young	< 0.04	1.5	0.5	< 9

Table 3

## Some General Data on Galaxies

Galaxy	$(m-M)_0$	Ref	$A_B$	Ref	$i$	$\sigma_r$	Ref	$f_V$	Ref
						km/sec			
M31	24.2	1	0.60	1	12.5	225	7	43	9
M32	24.2	1	0.60	1	0	98	7	6	9
M87	31.1	2	0.21	6	0	550	8	-	-
Fornax	22.0	3, 4	0.20	3	0	-	-	-	-
Sculptor	19.6	5	0.20	3	0	-	-	-	-

1. van den Bergh 1968

2. Sandage 1968

3. de Vaucouleurs, Ables 1968

4. Hodge 1961a

5. Hodge 1961b

6. Sharov 1963

7. Minkovsky 1962

8. Brandt, Roosen 1969

9. Spinrad 1971



Table 2

Parameters of Galactic Models

Galaxy	$M$	$L_g$	$\alpha$	$\epsilon$	$f_B$	$B-V$	$U-B$	$\log\langle\varrho\rangle$	$\log P(\varrho)$	$B(\varrho)$	$N$	$x$
Populations	$10^6 \odot$	$10^9 \odot$	kpc					$\odot \text{pc}^{-3}$	$\odot \text{pc}^{-3}$			
<b>Galaxy</b>												
Spheroid	35		0.9	0.60							4	10.5
Disc	95		6.4	0.10							1	1.5
Young	13		8	0.02							1	1.5
Total	143											
<b>M31</b>												
Nucleus	0.1		$5 \times 10^{-3}$	0.90	48	0.89	0.67	5.19	6.64	14.6	2	3
Kernel	0.3	$6 \times 10^{-3}$	0.15	0.90	48	0.89	0.65	2.73	5.78	16.8	4	7
Core	27	0.6	0.8	0.90	14	0.85	0.47	0.78	4.57	18.5	4	7
Bulge	46	3.3	3.0	0.30	3	0.65	0.16	-0.83	3.05	20.7	4	7
Halo	20	6.2	9.2	0.08	11	0.82	0.43	-1.27	2.46	23.5	1	1
Disc	85	7.5	8.0	0.02	3	0.33	-0.17	-1.55	1.40	24.6	0.5	0
Young	6	2.5			9							
Total A	185	20			18							
Total B	370	20										
<b>M87</b>												
Kernel	15	0.1	0.03	1.00	110	1.03	0.71	4.49	6.77	15.2	2	3
Core	1090	10	1.4	0.98	110	1.03	0.71	1.41	5.47	18.4	4	7
Bulge	1510	50	10	0.90	30	0.88	0.58	-0.99	3.89	21.0	4	7
Halo	226	70	76	0.35	3	0.60	0.05	-4.05	1.30	25.0	4	7
Total A	2840	130			22							
Total B	23000	130			170							
<b>M32</b>												
Kernel	0.05	0.01	0.003	0.8	6	0.87	0.38	4.05	6.25	13.3	2	3
Bulge	0.91	0.19	0.04	0.8	5	0.84	0.34	3.03	5.77	15.1	4	7
Halo	0.65	0.20	0.20	0.8	3	0.65	0.05	0.79	3.92	18.5	4	7
Total	1.61	0.40			4							
Fornax	106	106			3	0.65	0.05	-2.18	1.34	24.9	0.5	0
Halo	72	24	0.90									
<b>Sculptor</b>												
Halo	4	1.2	0.36	0.65	3	0.65	0.05	-2.21	1.02	25.0	1.5	1

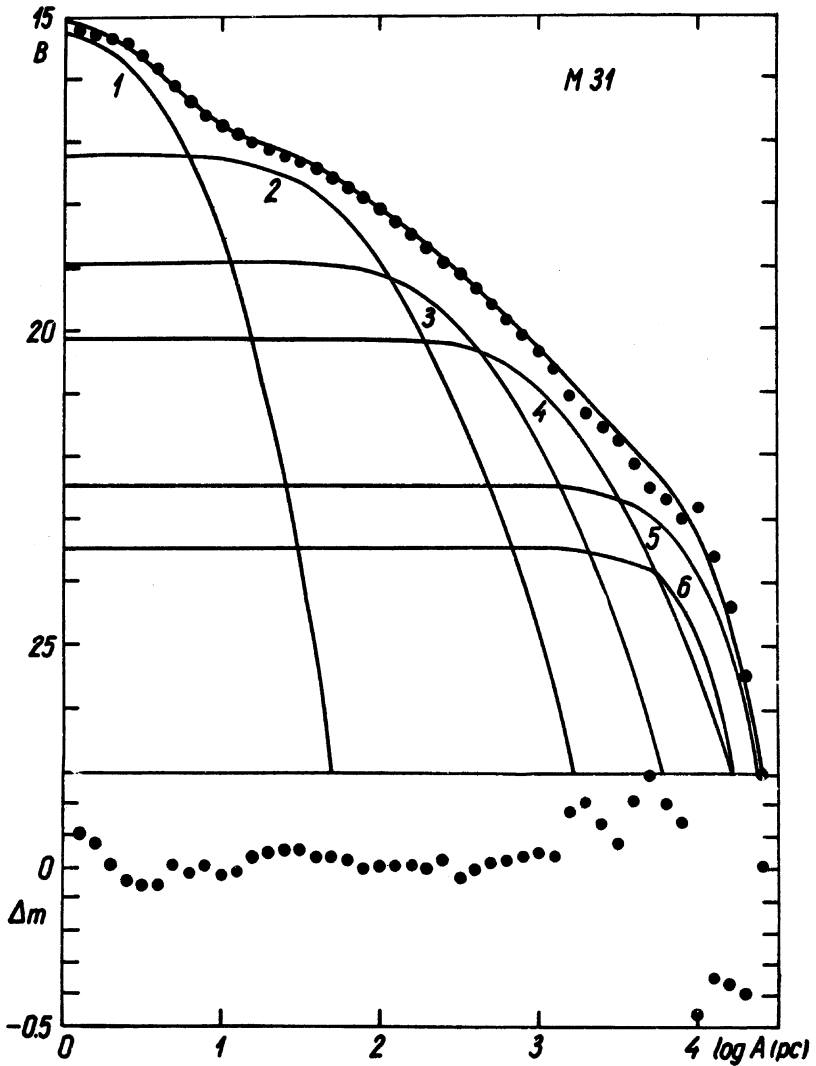


Fig. 1. The luminosity profile along the major semi-axis of M31. Dots represent observations compiled by Einasto (1969a), curves represent various components (1: kernel, 2: core, 3: bulge, 4: halo, 5: disc, 6: young population). In the lower part of the figure the deviations of the model from observations are shown.

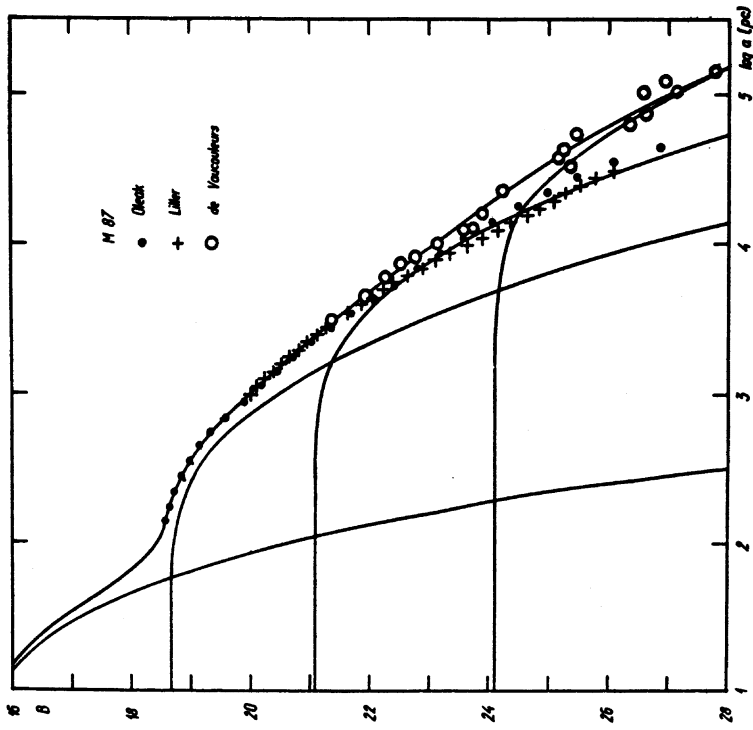


Fig. 2. The same as Fig. 1 for M87. Observations of various authors are plotted by different signs: Oleak (personal communication), Liller (1960), de Vaucouleurs (1969). At large distances from the centre photometric observations (Oleak, Liller) deviate from photoelectric ones (de Vaucouleurs), which indicate the presence of scale errors in photographic observations. Curves indicate the following components (from left): kernel (not visible due to large distance of M87), core, bulge, and halo.

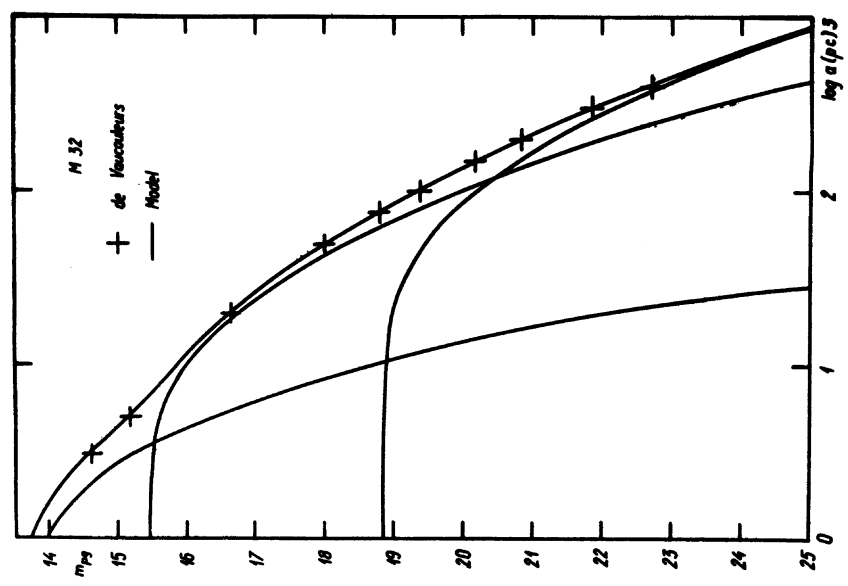


Fig. 3. The same for M32. Observed profile is taken from de Vaucouleurs (1953), the components are (from left): kernel, bulge and halo.

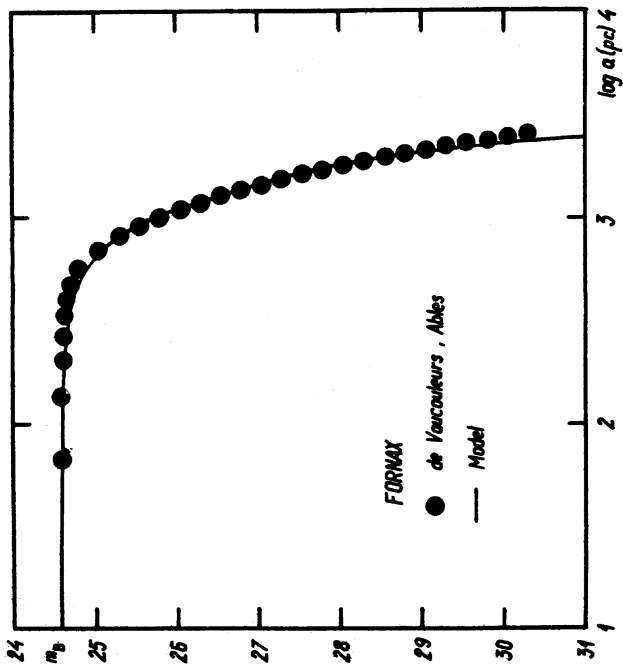


Fig. 4. The same for the Fornax galaxy; observations are taken from de Vaucouleurs and Ables (1968).

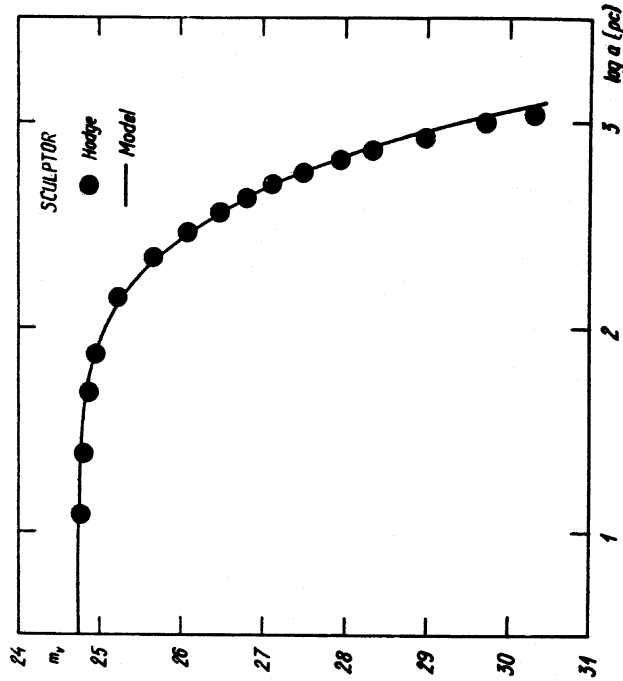


Fig. 5. The same for the Sculptor galaxy. Luminosity profile is derived from star counts (Hodge 1961b).

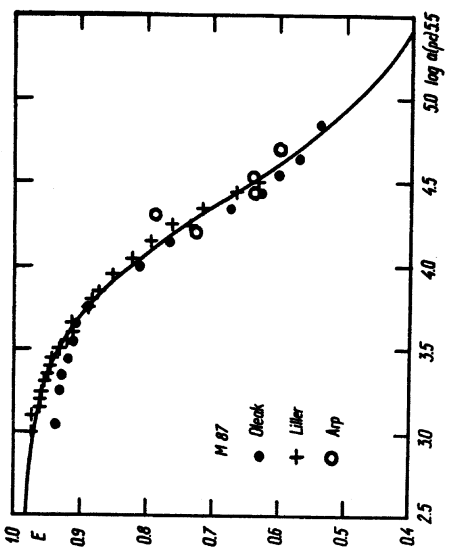


Fig. 7. The same as in Fig. 6 for M87. Observed axial ratios are taken from Oleak (personal communication), Liller (1960) and Arp and Bertola (1969).

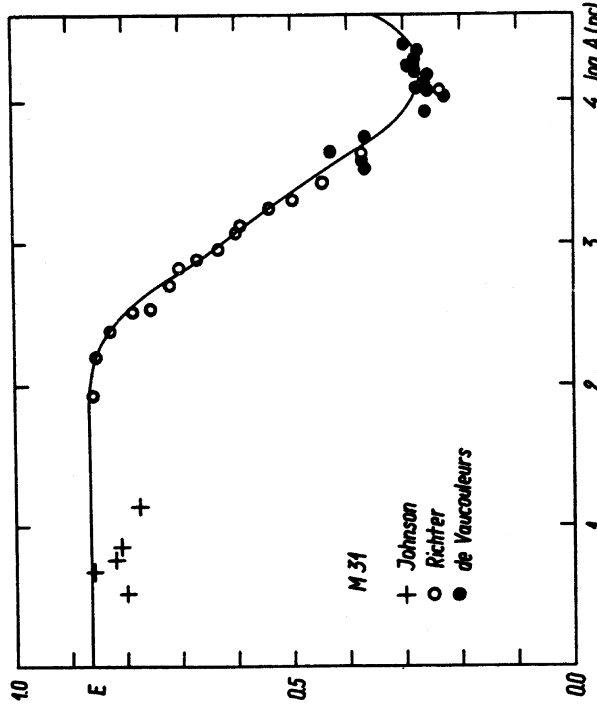


Fig. 6. The apparent axial ratio of equidensity ellipses as a function of major semi-axis for M31. Curve represents the model, observed values are taken from Johnson (1961), Richter and Hogner (1963) and de Vaucouleurs (1958).

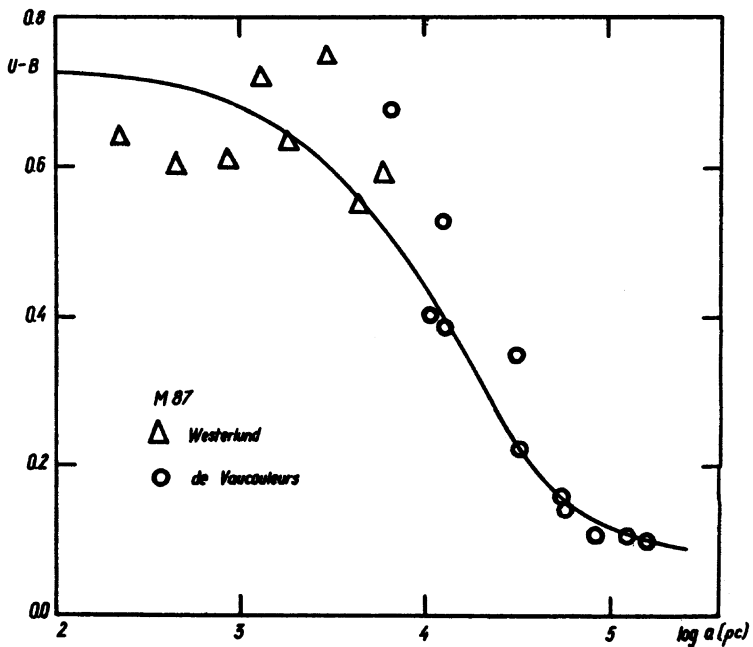
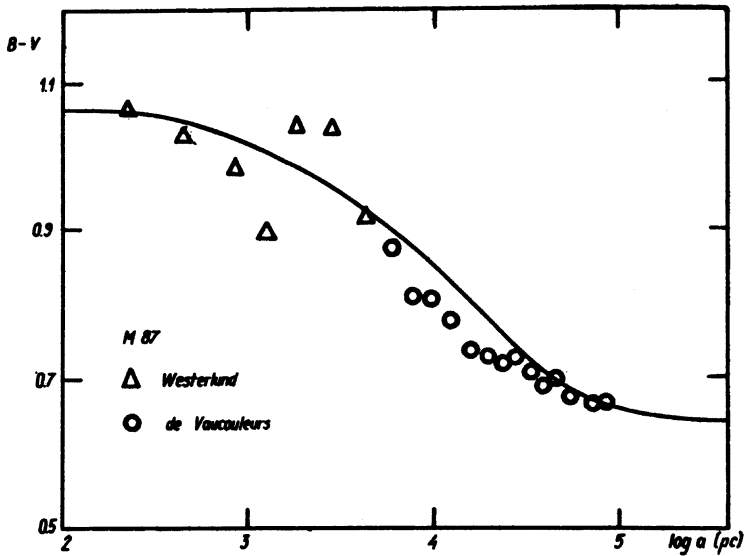


Fig. 8. The colour variations in M87. Curves represent the model, observed values are taken according to Westerlund and Wall (1969) and de Vaucouleurs (1969).

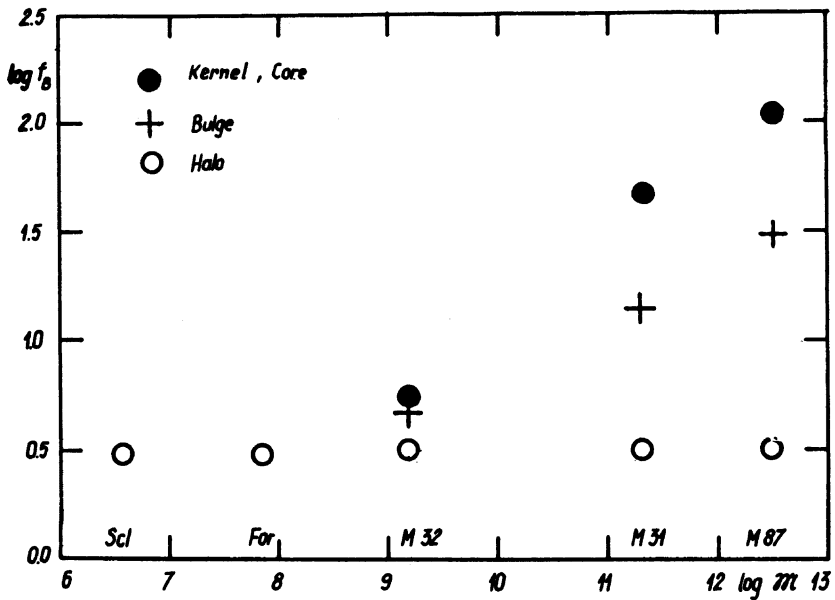


Fig. 9. The dependence of mass-to-luminosity ratios of old galactic components on the total mass of the galaxy  $M$ .

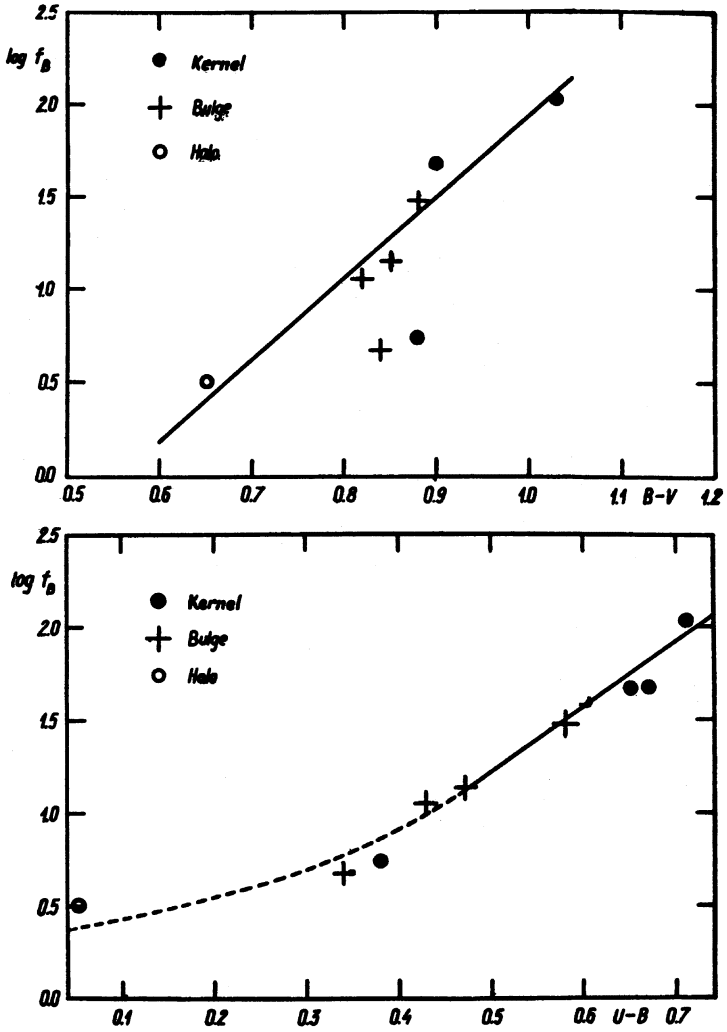


Fig. 10. The dependence of mass-to-luminosity ratios  $f_B$  of old galactic components on its  $B-V$  and  $U-B$  colours.



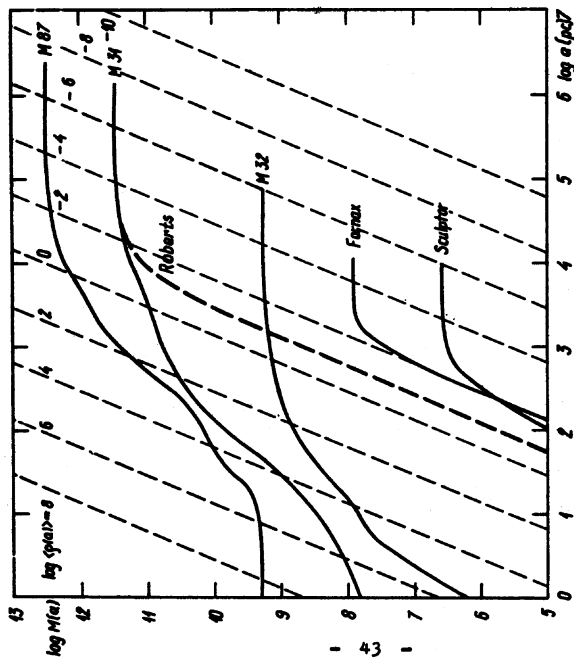


Fig. 11. The general mass distribution of galaxies MB7, M31, M32, Fornax, and Sculptor. For the Abdrameda galaxy, M31, the mass distribution according to Roberts (1966) model is given for comparison. The lines of constant mean inner density are given for the spherical distribution of mass. Mass is given in solar units, distance in parsecs.

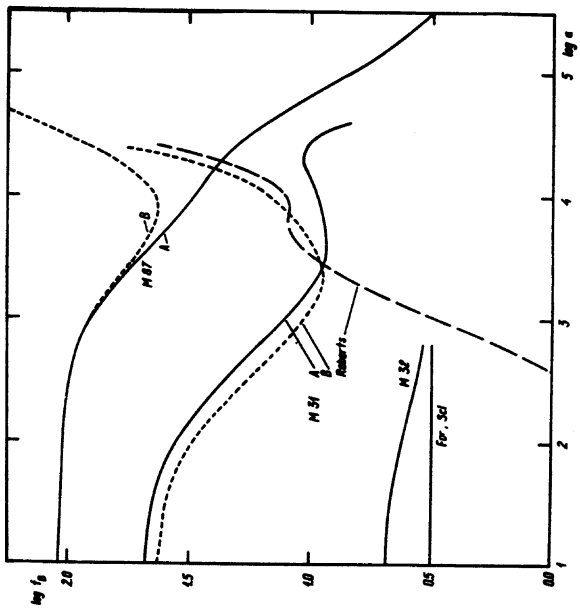


Fig. 12. The distribution of the projected mass-to-luminosity ratio for galaxies MB7, M31, M32, Fornax, and Sculptor. For galaxies MB7 and M31 the distribution is calculated for two models: A (without corona), and B (with corona). For M31 the distribution is given also according to the Roberts (1966) model.

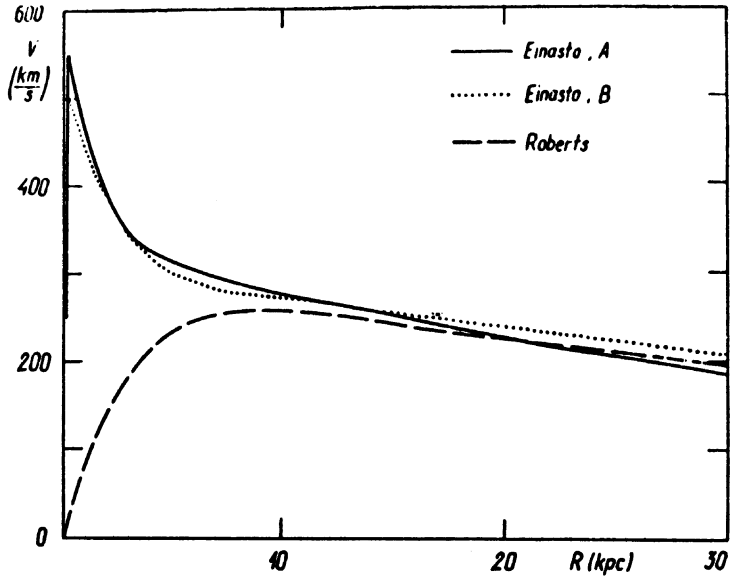


Fig. 13. The distribution of circular velocity of the Andromeda galaxy M31 according to the Einasto models (A without, and B with the corona), and Roberts (1966) model.

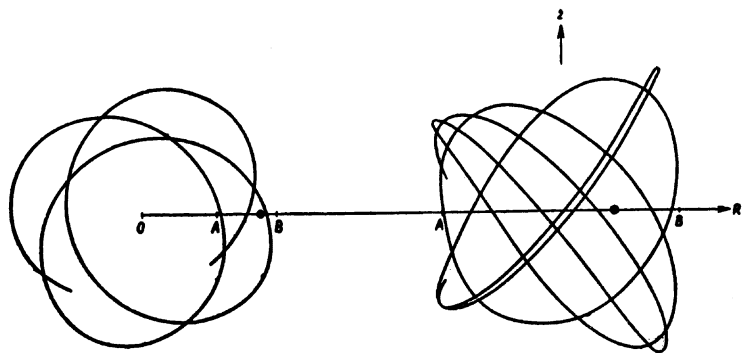


Fig. 14. Vertical (left) and meridional projections of a three-dimensional orbit of a star, calculated in 1953 by Belsalu. The points A and B corresponds to the minimal and the maximal distance of the orbit from the galactic centre at the equatorial plane of the Galaxy (reproduced from Kuzmin 1969).

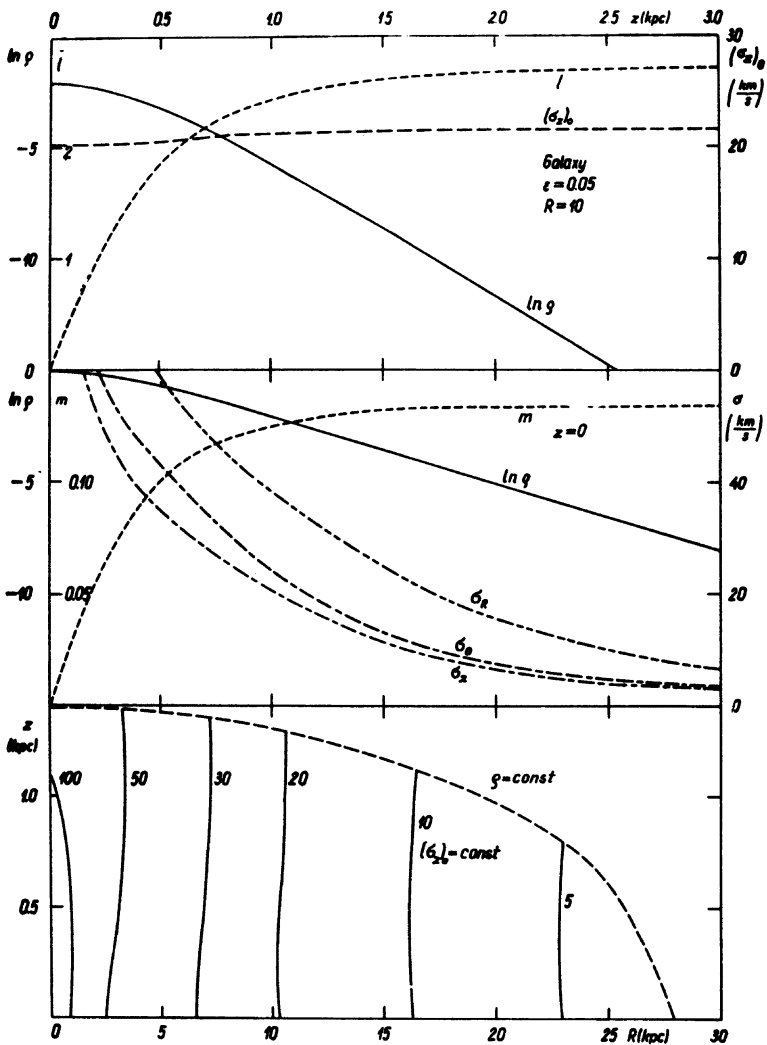


Fig. 15. Various descriptive functions of a test-populations of the Galaxy with the mean radius  $\alpha_0 = 7.4$  kpc, axial ratio  $\epsilon = 0.05$  and structural parameters  $N = 1$  and  $\kappa = 1.5$ . In the upper part of the Figure for  $R = 10$  kpc the dependence of the density  $\rho$  (in units of the central density  $\rho(0)$ ), vertical density gradient  $l = -\partial \log \rho / \partial z$  and velocity dispersion  $(\sigma_z)_0$  in Jeans approximation on  $z$  (s. Einasto 1970) are given. In the middle of the Figure the  $R$ -dependence of the density  $\rho$ , radial density gradient  $m = -\partial \log \rho / \partial R$  and of three velocity dispersions  $\sigma_R$ ,  $\sigma_\theta$ ,  $\sigma_z$  are shown for the galactic plane  $z = 0$ . In the lower part of the Figure the lines of constant density  $\rho$  and velocity dispersion  $(\sigma_z)_0$  are given. Velocities are expressed in km/sec.

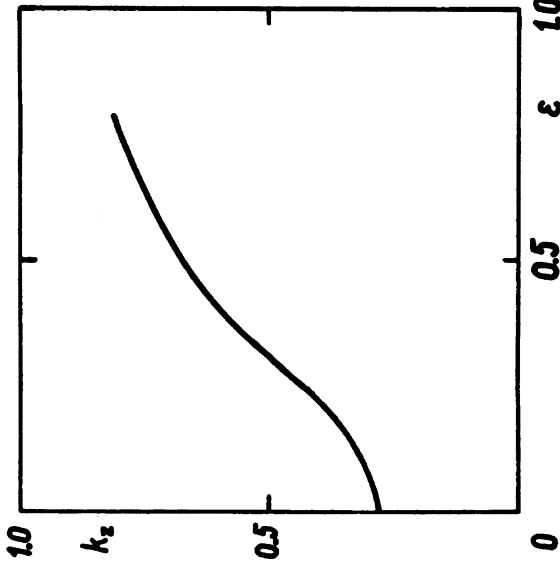


Fig. 16. The dependence of the axial ratio of the velocity ellipsoid  $k_2 = \sigma_x^2 / \sigma_y^2$  on the flattening parameter  $\epsilon$  of Galactic subsystems for the solar vicinity.

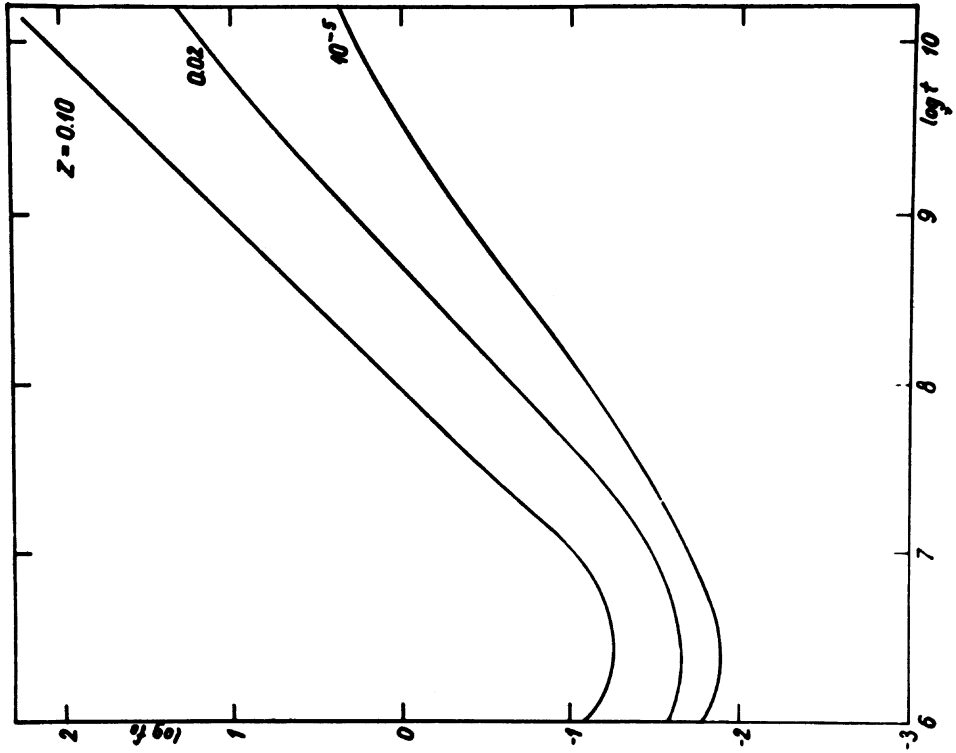


Fig. 17. The dependence of the mass-to-luminosity ratio of stellar populations of various heavy elements content  $Z$  on the age  $t$  (in years) of the population.

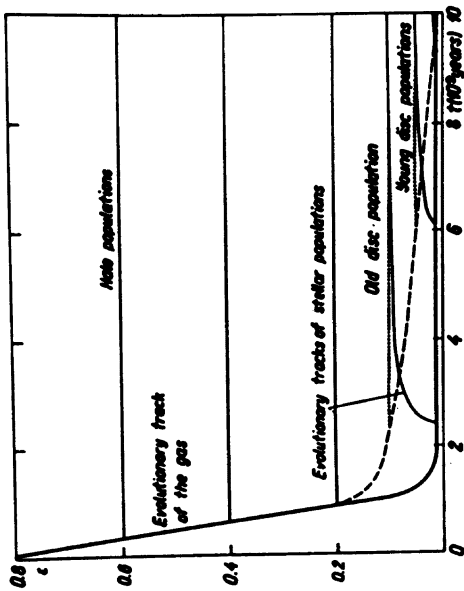


Fig. 18. Possible evolutionary changes of the axial ratio of equidensity ellipsoids  $\epsilon$  for the gas and stellar populations of different ages. Halo subsystems ( $f = 0.70$ ) have probably conserved their initial  $\epsilon$  values, but the axial ratio of disc subsystems increased due to the action of irregular forces. An alternative picture (the independence of  $\epsilon$  for all stellar populations) is shown by dashed (gas) and dotted (stars) lines. Reproduced from Elmasto (1977).

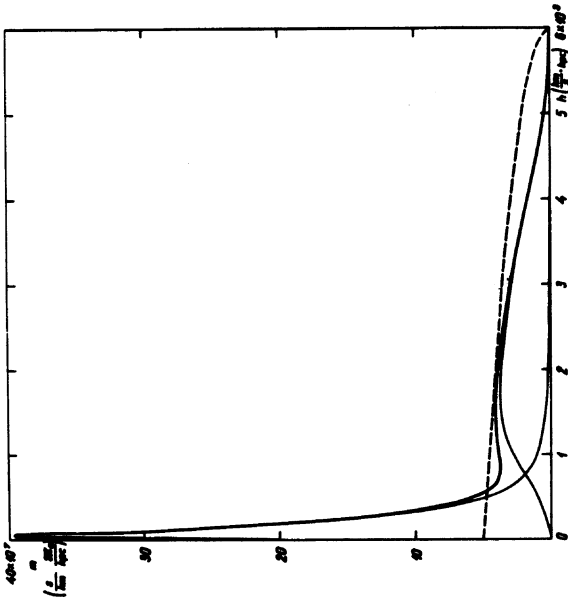


Fig. 19. The distribution of mass versus angular momentum  $h$  for the Andromeda galaxy M31. Thin lines correspond to spherical (core, bulge, halo) and disc populations, the thick one to the galaxy in general. The corresponding distribution for homogeneous spheroid, rotating with constant angular velocity, is indicated by a dashed line. The masses and maximal values of angular momenta of both models are identical.

### Errata

Tartu astr. obs. Tetaed No. 40, 1972

Page 28 9th row from below instead of "Otherwise we suppose..." it should be read "In other words we suppose...".

Page 34 Table 3. For galaxies M87, Fornax and Sculptor instead of the true distance moduli  $(m - M)_0$  the apparent moduli  $(m - M)_B$  are given.

Note: in the final version of the report, to be published in the Proceedings of the First European Astronomical Meeting, the term nucleus is used for the central dense star cluster, and the term kernel for the central quasipoint mass, responsible for the activity of the galaxy. Some other minor changes have also been made. All numerical results have remained unchanged.